



Research Article

Critical investigation of microchannel design effect on thermal performances of a pem fuel cell

Khaoula KHELAIFA¹, Abdelmalek ATIA^{1,2,*}, Hocine Ben MOUSSA³, Ammar NAROURA¹

¹LEVRES Laboratory, University of El Oued, El Oued, 39000 Algeria

²UDERZA Unit, University of El Oued, El Oued, 39000 Algeria

³Faculty of Technology, University of Batna-2, El Oued, 50000 Algeria

ARTICLE INFO

Article history

Received: 10 September 2022

Accepted: 25 December 2022

Keywords:

PEMFCs; CFD; Nanofluid, Cooling Plate; Microchannel; Heat Transfer

ABSTRACT

A major challenge for improving the characteristics of fuel cells is to obtain uniform temperature distribution during its operation, in which a major part of hydrogen chemical energy is converted to heat. If not properly exhausted, this exothermic chemical reaction causes overheating in the polymer electrolyte membrane fuel cells (PEMFCs), leading to a reduction in their performance. Hence, analyzing different techniques for PEMFCs cooling may be necessary for this kind of energy systems. In this study, four microchannel design effect on aluminum oxide (Al_2O_3) nanofluids thermal behavior in cooling plates with 1400×1800 mm² was investigated using computational fluid dynamic (CFD) simulation. The performances of proposed microchannel designs were evaluated in terms of maximum and uniformity temperature. The suggested study has been validated by available published results from previous research studies. The obtained results depicted that the maximum temperatures have been 305.3K and 305.5K for S- character flow field and two stages coolant flow field microchannel designs, respectively. The results revealed that the multi-flow plate designs might greatly enhance the performance of PEMFCs in terms of temperature distribution in the cooling plate when compared to standard flow field designs. Another important finding was that the two stages microchannel and S-design are more thermal stable compared with other microchannels.

Cite this article as: Khelaifa K, Atia A, Moussa HB, Naroura A. Critical investigation of microchannel design effect on thermal performances of a pem fuel cell. J Ther Eng 2024;10(1):36–49.

INTRODUCTION

The global energy crisis is one of the most challenging issues; the continuously increasing energy consumption is mainly met by a limited reserve of fossil fuels which causes environmental problems [1-3]. Thus, the researchers have been seeking new resources in alternatives to the fossil

fuels, where attention is drawn to the development of sustainable and clean renewable energies such as solar thermal energy, photovoltaic cells, wind energy, hydropower, geothermal, biofuel energy [4, 5].

Fuel cells are one of the most effective techniques for producing electricity in a clean way. In these systems,

*Corresponding author.

*E-mail address: abdelmalek-atia@univ-eloued.dz

This paper was recommended for publication in revised form by Regional Editor Müslüm Arıcı



chemical energy of fuels such as hydrogen can be converted into electrical energy directly, without going through mechanical energy. There are several types of fuel cells that can be classified according to the nature of the electrolyte (a material that contains free ions that form a transportable or its operating temperature [6, 7]). These types include proton transport membrane fuel cells. Since the PEM fuel cell is an advanced technology, its development still faces many problems that must be addressed. Many economic, scientific, and technological aspects must be accurate and ideal in order to obtain a viable technology, such as cost, durability, and reliability of the cell and the flow of water and heat in it. To overcome these problems, many research activities have been carried out during the past three decades [8, 9]. These studies are generally classified into two categories: experimental and numerical simulations. The investigation of using silicon dioxide and aluminum oxide in water as cooling fluid in PEMFC is the central point of work that carried out by Zakaria et al. [10]. The authors used ANSYS Fluent to study thermal behavior of laminar flow of the proposed nanofluid with low concentration value of silicon dioxide and aluminum oxide below to 0.5 % was adopted. This work indicated that the enhancement of heat transfer coefficient reached to 2.14 % via aluminum oxide utilization and 1.15 % by using silicon dioxide in the concentration of 0.5 % as compared to water.

A recent study by Khalid et al. [11] examined nine mixture ratios of Al_2O_3 - SiO_2 fluctuating from 10:90 to 90:10 for advanced coolant application in PEMFC. The findings of this study depicted that the successive increases in the percentage of Al_2O_3 leads to increase of the dynamic viscosity the coolant fluid. Meanwhile the electrical and thermal conductivity moved further to decrease. Arear et al. [12] proposed a simulation model to investigate heat transfer in the PEMFC with nanoparticles Al_2O_3 . The authors demonstrated that the use of nanofluid contribute in the enhancement of PEMFC cooling process. In addition, the increase of nanoparticles concentration is associated with the increase of pressure drop and pumping power. Four hybrid ratios of Al_2O_3 - SiO_2 nanofluids were proposed by Johari et al. [13] for cooling PEMFC. They demonstrated that the property of heat conductivity was improved by up to 21.2% as compared to the base fluid.

The cooling of polymer membrane FC using nanofluids was carried out by Kordi et al. [14]. In this study, the augmentation of nanoparticle ratio by 0.6% were found to cause the decrease of temperature uniformity index and increase the pressure drop about 13 % and 35 %, respectively. Afshari et al. [15] investigated 3D numerical simulation about temperature distribution in the PEM fuel cell using straight and serpentine flow field. However, the observed difference between the two models in terms of uniformity index and temperature difference in this study was not significant, however, the pressure drops in the serpentine model is more than that found in straight model. As shown by Saeedan et al. [16], utilization of metal foam

within the channels leads to enhance the characteristics of a PEMFC in terms of temperature uniformity index, maximum temperature. An important issue that emerged with the use of metal foam is the increase in pressure drops in the system about 4.4%.

Mahdavi et al. [17] proposed metallic bipolar plates design for cooling a PEM fuel cell by using water-based nanofluid with a concentration of 5 %. The simulation results show that the desired cooling performance is achieved at Reynolds number of 500, which is reduced to a half if compared with the base fluid. Also, the innovative cooling design employed in the study is presented to exquisitely contract the size of fuel cell. Used The hybrid Al_2O_3 - SiO_2 as a coolant in the distributor cooling plate of a PEMFC was presented by Idris et al. [18]. Their findings depicted that the ratio of 10:90 Al_2O_3 - SiO_2 is the most optimal hybrid nanofluid at the Reynolds number of 1000. Furthermore, the exploitation of hybrid nanofluids enhance coolant fluid properties and thermal management potential in PEM Full Cells. Ogura et al. [19] developed a new small PEMFC system where the system was designed using the simulation of a chemical reaction and thermal transfer to obtain a sufficient hydrogen production rate and a suitable temperature distribution for methanol-reforming. This device generated an output of approximately 2.5W with sufficiently low heat loss. The size of the fuel cell makes this system suitable to apply as a power source for mobile devices.

Chugh et al. [20] experimentally studied PEM fuel cell stack employing Nafion®-212. The investigation of operating parameters influence on the fuel cell performance was carried out. Beside the experimental work, the authors compared the obtained results with those of mathematical model developed in MATLAB under steady state conditions. A 3D numerical model of two phases flow in a single serpentine channel polymer electrolyte membrane fuel cell under ANSYS Fluent simulation was used to investigate the pressure effects on the PEMFC performance. A series of experiments was done for validating the developed numerical model [21]. Chun et al. [22] studied the influence of gas diffusion layer (GDL) properties on the PEMFC performances by both numerical simulation and experiments. They found that the GDL properties greatly influence on the cell performances.

A sinuous flow field channel was experimented for PEMFC performances and water management improving [23]. This work addressed at cathode side through both numerical and experimental investigation, by scaling up of fuel cell from 25 to 100 cm^2 . The results showed that the power loss in sinuous flow field channel caused by scaling was only 24.44%. In experimental studies, research usually focuses on improving cell performances, but the combination of temporal and spatial scales by means of experimental methods is still challenging since the measure of the length of the basic elements of the cell ranges between micro and macro, and the time scale for some transfers ranges from milliseconds to a few hours [24], hence physical models

can be costly and time consuming. Consequently, fuel cell modeling and simulation has become a practical and useful method for researchers, for improving the design of a less expensive and more efficient fuel cell.

One of the significant factors affecting the performance of a PEM fuel cell is the formation of cold plates. Improving the geometrical parameters of the coolant flow channels (fluid having the advantage of removing excess heat from the cell) such as the dimension (width, length, and depth) or the cross-section shape of the channel can augment the performance of the fuel cell. The aim of this work is to investigate the heat transfer phenomenon by CFD analysis for studying the effect of the channel plate design on the performance of the PEM fuel cell. Furthermore, this paper assesses the significance of using two stages straight microchannel with co-current and counter-current fluid flow as cooling plate for PEM fuel cell. This investigation will contribute to a deeper understanding of the effect of two stages microchannel compared to one stage microchannel in the sector of PEMFC performances enhancement. Al_2O_3 -water ethylene glycol and SiO_2 in desalted water mixture nanofluids were used as a working fluid in the present study.

PHYSICAL MODEL AND HYPOTHESES

The mass and heat transfer equations can be changed, from one component to another in a fuel cell, i.e., each component of the cell has its own mathematical equations. However, we show the case of transport phenomenon modeling in the PEM fuel cell for cooling plate element.

The 3D CFD dynamic model was established based on the dimensions of a particular cooling plate as presented in Figure 1. The cooling plate for PEM fuel cells consists of multiple simultaneous channels with the following dimensions: 5 mm x 1 mm x 140 mm, where the plate has been subjected to significant heat load of 100 watts.

A significant amount of research work on fluid flow and convective heat transfer in very thin channels has been

published in recent literature, due to the miniaturization in the design of PEM fuel cell components, which plays a very important role in achieving of high energy densities [25-28]. Hence, it is desirable to have these channels in the active thermal transport environment of electrolytic. The mini-channels contribute also to augment the heat and the mass transfer rates that leads to the lowering of the maximum cell temperature compared to the micro channels [24]. The materials used for the flow channels, to manufacture the cooling plate is graphite carbon. So far, several forms of nanofluid flow channels have been designed. Improving the PEM fuel cell performances requires more efficient cooling systems, beside several studies, it has been observed that the cooling using carbon-graphite plates, in which channels for the nanofluids flow is more efficient in order to cool the fuel cell. Here it may be concluded that the shape of channels and the nature of the nanofluids flow have a very important role for improving the cell performance, i.e., a significant reduction of T_{max} and a uniform temperature distribution. For this purposes, various configurations for the nanofluid flow channels have been proposed and studied via CFD simulation. Figure 2 illustrates four different designs of the flow channels. Most studies of microchannel cooling plate design effect have only been carried out in one stage and simple way of fluid direction.

The physical and thermal parameters of one and two stages straight plate used for the numerical simulation in this work are listed in Table 1.

In order to simplify the analysis, some assumptions are considered:

- Fluid properties are constant, steady state fluid flow, incompressible and laminar flow;
- The effects of the fluid force and viscous dissipation on the channels are ignored;
- The base liquid nanoparticles W / EG and Al_2O_3 in thermodynamic equilibrium at zero relative speed and resulting mixture may be regarded as a single standard phase;

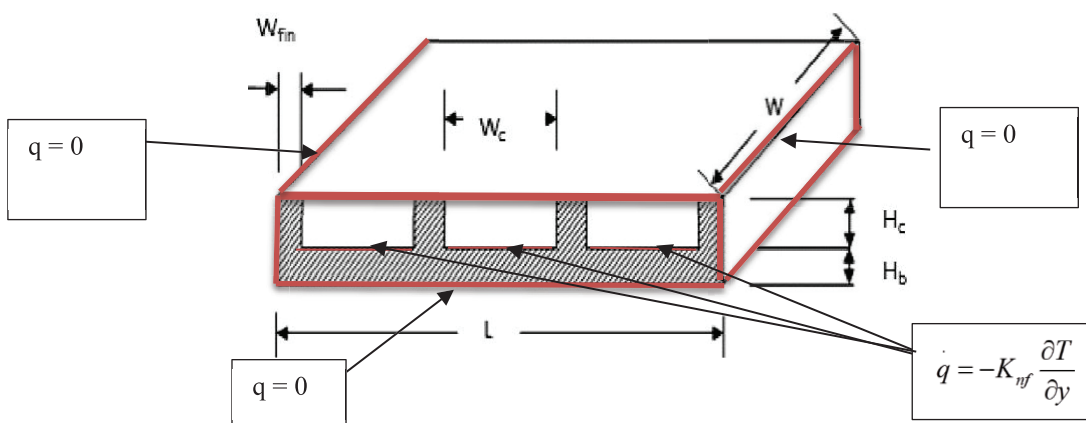


Figure 1. Schematic diagram of the microchannel in the PEMFC cooling plate.

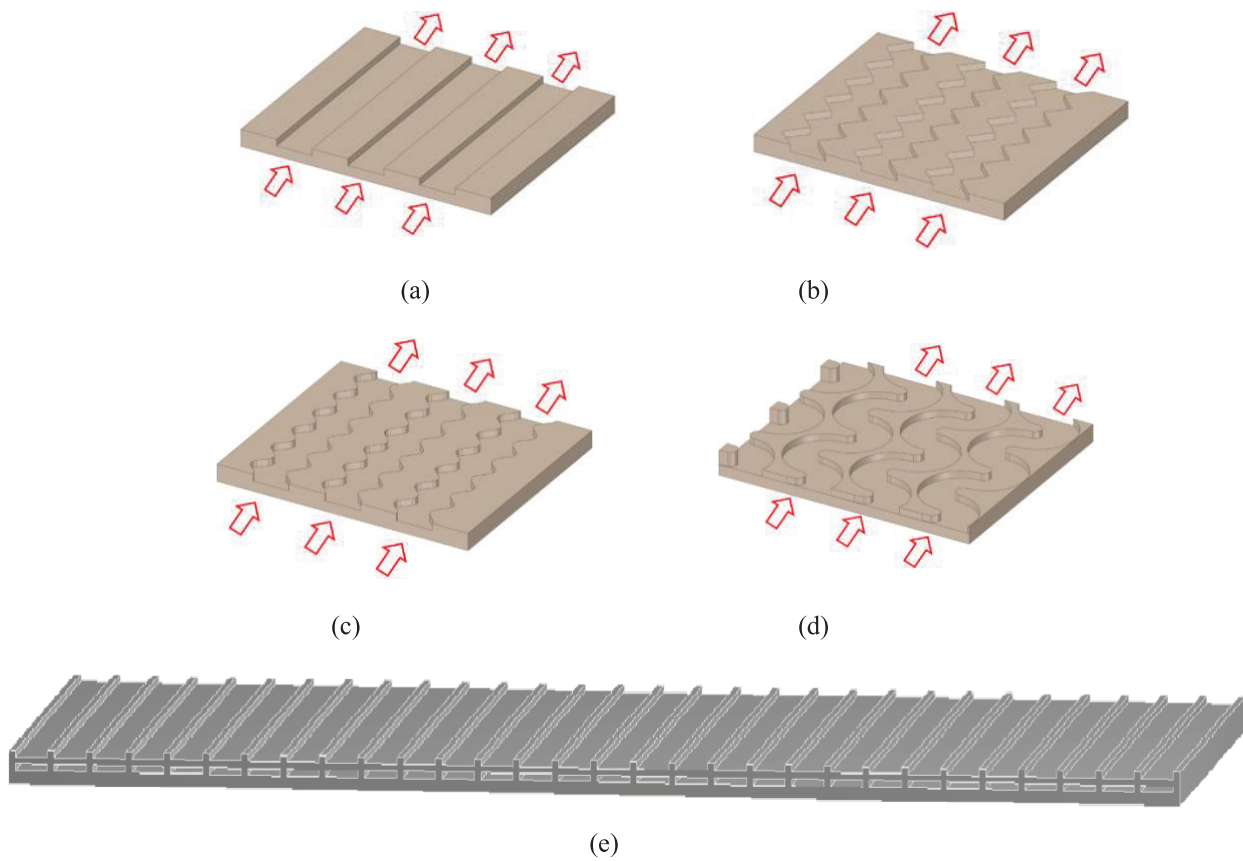


Figure 2. The fluid flow channels configurations for the PEMFC cooling plate, (a) one stage straight, (b) normal Zigzag, (c) curved zigzag, (d) S-shaped and (e) Proposed solution: two stages straight plate.

Table 1. Coefficients, physical properties, and operating conditions used for one and two stages straight plate [12, 13, 24]

	Coefficients and properties	One stage straight plate	Two stages straight plate
Dimensions of the cooling plate	Plate length L_p	181 mm	181 mm
	Plate width W_p	150 mm	150 mm
	Plate Height H_p	2.5 mm	2.5 mm
	W_{fin}	1 mm	1 mm
	Channel width W_c	5 mm	5 mm
	Channel depth H_c	1.5 mm	0.5 mm
	Hydraulic diameter D_h	0.00231 mm	0.00091 mm
Plate properties (graphite)	Density ρ	2250 kg/m ³	2250 kg/m ³
	Specific heat C_p	690 J/kg. K	690 J/kg. K
	Thermal conductivity K_s	24 W/m. K	24 W/m. K
Fluid 1: (Al ₂ O ₃ -W / EG Mixture) 0.5%	Density ρ	1071.432 kg/m ³	1071.432 kg/m ³
	Specific heat C_p	3440.9 J/kg. K	3440.9 J/kg. K
	Thermal conductivity K_{mf}	0.463 W/m. K	0.463 W/m. K
	Dynamic viscosity μ	0.003187 Pa.s	0.003187 Pa.s
Fluid 2: (SiO ₂ in desalted water) 0.5%	Density ρ	1365.3 kg/m ³	1365.3 kg/m ³
	Specific heat C_p	4142.065 J/kg. K	4142.065 J/kg. K
	Thermal conductivity K_{mf}	0.617 W/m. K	0.617 W/m. K
	Dynamic viscosity μ	0.002128 Pa.s	0.002128 Pa.s
Operating conditions	Heat flow rate q (W/m ²)	4000,6000,8000,10000,12000	4000,6000,8000,10000,12000
	Internal fluid temperature T_{in}	300 K	300 K

- All the channel of the cooling plate are identical in terms of heat transfer and flow property of the nanofluids.

Mathematical Formulation and Boundary Conditions

Some assumptions are made for the analysis of three-dimensional flow. Laminar and steady flow is considered. The fluid is supposed Newtonian and incompressible. A governing equations including momentum, energy, and mass equations for the considered problem can be expressed in Cartesian coordinates as follows [25]:

$$\frac{\partial u}{\partial x} + \frac{\partial v}{\partial y} + \frac{\partial w}{\partial z} = 0 \quad (1)$$

$$\rho \left(u \frac{\partial u}{\partial x} + v \frac{\partial u}{\partial y} + w \frac{\partial u}{\partial z} \right) = -\frac{\partial P}{\partial x} + \mu \Delta u$$

$$\rho \left(u \frac{\partial v}{\partial x} + v \frac{\partial v}{\partial y} + w \frac{\partial v}{\partial z} \right) = -\frac{\partial P}{\partial y} + \mu \Delta v \quad (2)$$

$$\rho \left(u \frac{\partial w}{\partial x} + v \frac{\partial w}{\partial y} + w \frac{\partial w}{\partial z} \right) = -\frac{\partial P}{\partial z} + \mu \Delta w$$

$$u \frac{\partial T}{\partial x} + v \frac{\partial T}{\partial y} + w \frac{\partial T}{\partial z} = \frac{K_{nf}}{\rho c_p} \Delta T \quad (3)$$

For the solid region of the flow channel, the energy equation is given by:

$$\frac{\partial^2 T}{\partial x^2} + \frac{\partial^2 T}{\partial y^2} + \frac{\partial^2 T}{\partial z^2} = 0 \quad (4)$$

For boundary conditions, no sliding boundary condition on the wall, constant velocity at the entrance and atmospheric pressure at the outlet are applied.

$$\overline{V}_{wall} = 0$$

$$\overline{V}_{inlet} = 0 \quad (5)$$

$$P_{outlet} = P_{atm}$$

For this solid region (wall) of the nanofluid flow channel ($\text{Al}_2\text{O}_3\text{-W}$ / EG mixture), we considered the energy conservation equation as described in [24]

$$K_s \left(\frac{\partial^2 T}{\partial x^2} + \frac{\partial^2 T}{\partial y^2} + \frac{\partial^2 T}{\partial z^2} \right) = 0 \quad (6)$$

The heat is transferred through the solid and dissipated by the forced load of the nanofluid that passes through the flow channel, the bottom surface is heated regularly with a continuous heat flow where at the lower surface of the channel

$$q_{lower\ surface} = -K_{nf} \frac{\partial T}{\partial y} \quad (7)$$

The upper surface of the channel is adiabatic, so it is written as

$$q_{upper\ surface} = -K_{nf} \frac{\partial T}{\partial y} = 0 \quad (8)$$

The simulation of the thermal behavior described in this work was performed using finite volume method. The most several steps of numerical procedure, geometry creation, mesh generation, choose the initial and boundary conditions of your model for each physics used / select the appropriate material from the model, and macroscopic variables are calculated/ the desired results are shown. The informatics steps process is presented in Figure 3.

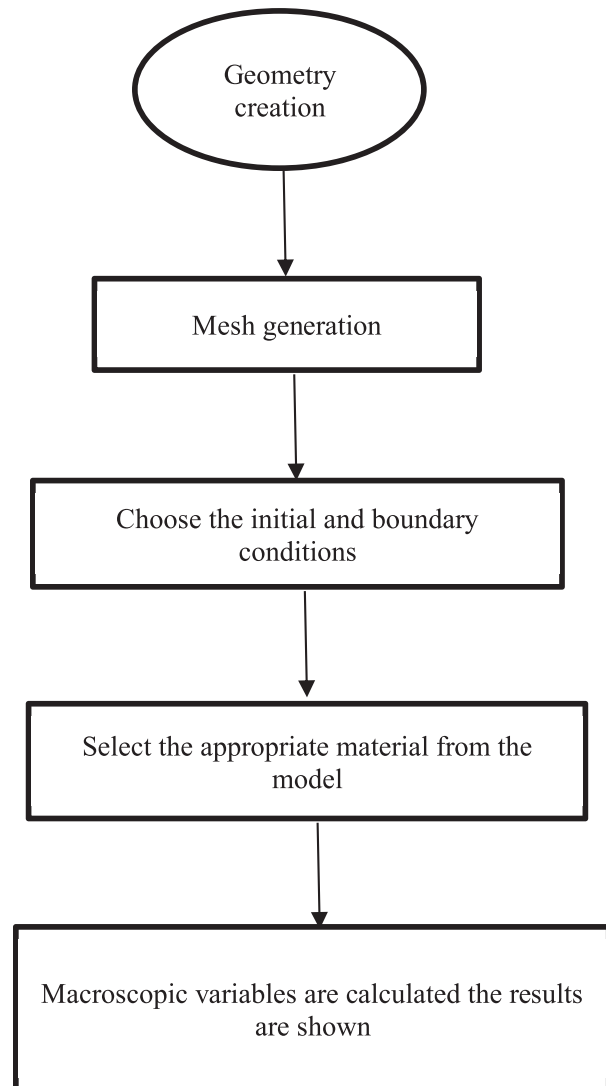


Figure 3. Simulation steps.

Table 2. Results validation

	ΔT (K)			T_{av} (K)			T_{max} (K)		
	Beak et al [26]	Present study	Relative error	Beak et al [26]	Present study	Relative error	Beak et al [26]	Present study	Relative error
$Q= 2 \times 10^{-6} \text{ m}^3/\text{s}$	39.843	38.608	3.09						
$Q= 4 \times 10^{-6} \text{ m}^3/\text{s}$	21.188	20.653	2.52						
$Q= 6 \times 10^{-6} \text{ m}^3/\text{s}$	14.696	14.925	1.56	322.964	323.948	0.3	314.363	314.662	0.1
	ΔP (Pa)			h (W/m ² . K)			Nu		
	Zakaria et al [24]	Present study	Relative error	Zakaria et al [24]	Present study	Relative error	Zakaria et al [24]	Present study	Relative error
Re=120	2170	1960	9.67	1224.561	1219.512	0.41	4.558	4.57	0.26
Re=100	1943.455	1813.265	6.69	1171.93	1112.49	5.07	4.364	4.12	5.59
Re=80	1791.273	1616	9.78	1100	1086.97	1.18	4.096	4.1	0.097
Re=60	1580.182	1502	4.95	1112.281	1124	1.053	4.143	4.2	1.38
Re=40	1467.273	1457	0.7	1107.018	1133.787	2.42	4.123	4.25	3.1
Re=20	1275.818	1158	9.23	1056.14	1114.1	5.49	3.949	3.85	2.5
	U_T (K)			ΔP (Pa)			ΔT (K)		
	Li and Sundén [27]	Present study	Relative error	Li and Sundén [27]	Present study	Relative error	Li and Sundén [27]	Present study	Relative error
Re=250	1.765	1.7	3.68	200.968	200.9443	1.18	8.283	7.902	4.59

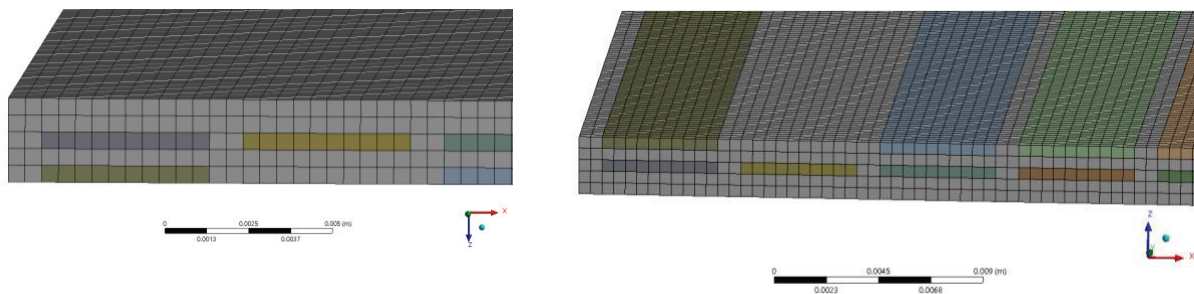


Figure 4. Mesh generation.

Model Validation

To verify our numerical present model, we first compared our results with those obtained by Beak et al. [26], Zakaria et al. [24], and Li and Sundén [27], which are displayed in Table 2. For fluid flow $2 \times 10^{-6} \text{ m}^3/\text{s}$, $4 \times 10^{-6} \text{ m}^3/\text{s}$ and $6 \times 10^{-6} \text{ m}^3/\text{s}$, the minimum and maximum relative error of difference temperature is 1.56% and 3.09% for Beak et al. [26] work compared with the present model. On other hand, the relative error of temperature average is 0.3% for $6 \times 10^{-6} \text{ m}^3/\text{s}$ while 0.1% for maximal temperature. At Reynolds number (Re) of 120 the relative error reached 9.67% for the drop pressure whereas 0.7% at Re of 50 compared between present work and Zakaria et al. [24] work.

Table 3. Mesh test for two stage counter-current

Number of elements	ΔP (Pa)	T_{max} (K)
74240	3187.37	307.084
168837	3238.85	306.638
243836	3260	306.741
313900	3279	306.604
405750	3297	306.578
543000	3312.45	306.552
916464	6426.19	305.454
1072560	6426.39	305.453
8855241	6426	305.482

The errors of coefficient convective are estimated 0.41% and 5.49% for Re of 120 and 20, respectively. In addition, the errors are reached 0.097% for Re =80 and 5.59% for Re = 100 at Nusselt number [28]. For parameter the uniformity temperature index (U_T), the drop pressure and difference temperature, the relative errors are estimated 3.68, 1.18 and 4.59, respectively at Re of 250.

Mesh test

A systematical mesh independence test is performed to demonstrate that the numerical findings are independent of the mesh number, where CFD simulation is used to build the designed mesh. Nine various mesh systems are generated for two stages straight plate counter-current fluid flow. The corresponding results of pressure drop and maximum temperature are displayed in Table 3. Therefore, the

number of elements) 916464 (is utilized for the numerical study. The average time required to reach the accurate solutions is about 30 min and the linear uniform mesh was used in the present simulation (Figure 4). The simulation results of this study were obtained by a PC has a Processor Intel® Core i5 CPU 2.27 GHz, RAM 8.00 GB and installed System of 64 bit.

RESULTS AND DISCUSSION

Heat transfer in nanofluids (Al_2O_3 -W / EG mixture) was investigated on the basis of both the convective heat transfer coefficient h and Nusselt number. The convective heat transfer coefficient variation is illustrated in Figure 5. The convective heat transfer improved with both volume concentration and number of Reynolds increasing. Design flow

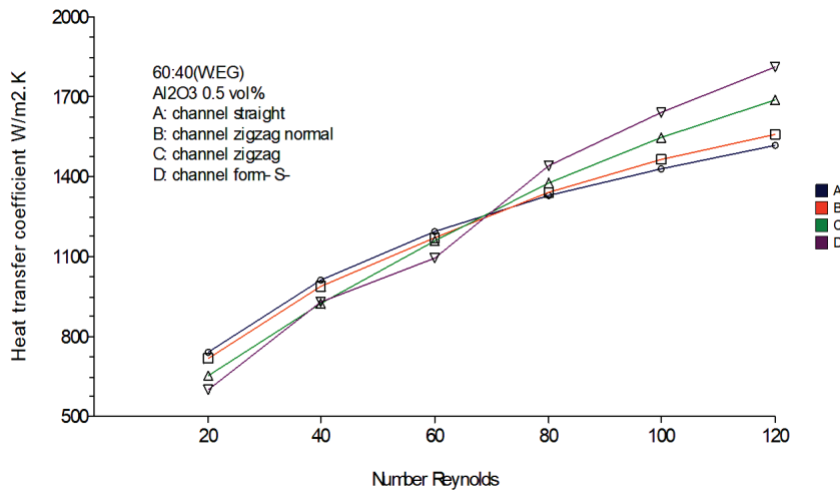


Figure 5. Heat transfer coefficient h for the four nanofluid models (Al_2O_3 -W (60) / EG (40) mixture).

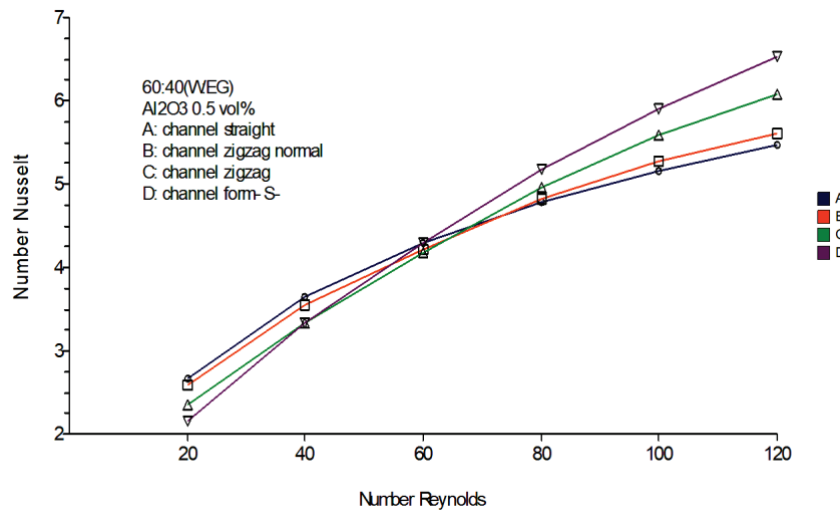


Figure 6. Nusselt number vs. Reynold number of the four models with nanofluid (Al_2O_3 -W (60) / EG (40) mixture).

channels (B, C, D) with the use of nanofluid (Al_2O_3 0.5vol% - W (60) / EG (40)) have a higher heat transfer coefficient, compared to the straight flow channel at Reynolds numbers greater than 70. Close to Reynolds numbers of 70 the, the heat transfer coefficient of the curved channels (B, C, D) is lower than the straight channel. The (S) form flow channel has the highest heat transfer coefficient with a boost rate of up to 19.3% compared to the straight channel. The shape of the geometry D path causes an increase in the arrival time of the fluid, which resulted in an increase in the value of the convective heat transfer coefficient at a high Reynolds number.

The coefficient convective heat transfer was used to evaluate the Nusselt number. In general, Nusselt number increased linearly with the number of Reynolds. From here,

the boundary channels effect (bends) of flow channels (B, C, D) are shown at Reynolds numbers greater than 60 as they outperform the straight channel due to the increase in the heat transport coefficient. The highest of Nusselt number in the S-channel compared to the straight channel has increased by additional 19.2% followed by the curved channel (C) with a reinforcement rate of 11.15%, followed by the broken channel (B) at 2.56% as shown in Figure 6.

Figure 7 depicts the variation of pressure drop versus Reynolds numbers ranging from 20 to 120 for all four configurations (A, B, C, and D). This figure presents a linear increase in pressure drop with inlet Reynolds number. A high-pressure drop was predicted, as the nanofluidic coolant had to travel through the cooling plate's narrow channels, the highest pressure drops at the curved channel (C)

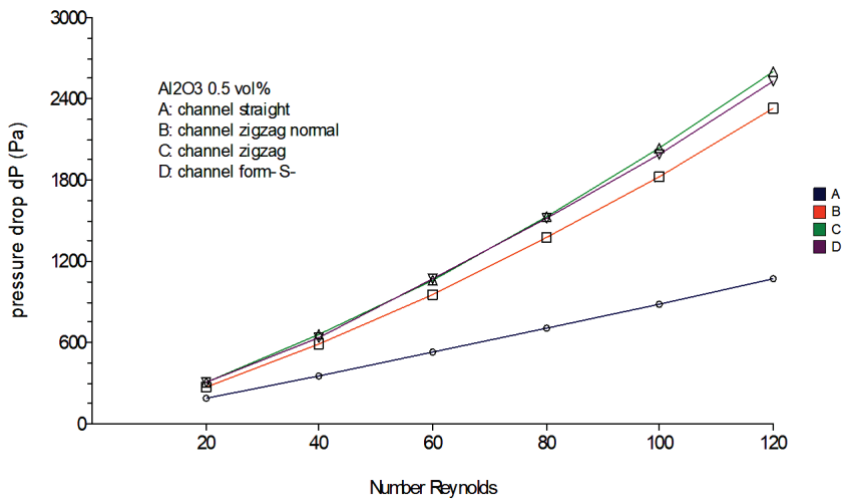


Figure 7. Pressure drop of the nanofluid (Al_2O_3 -W mixture (60) / EG (40)) versus Reynolds number.

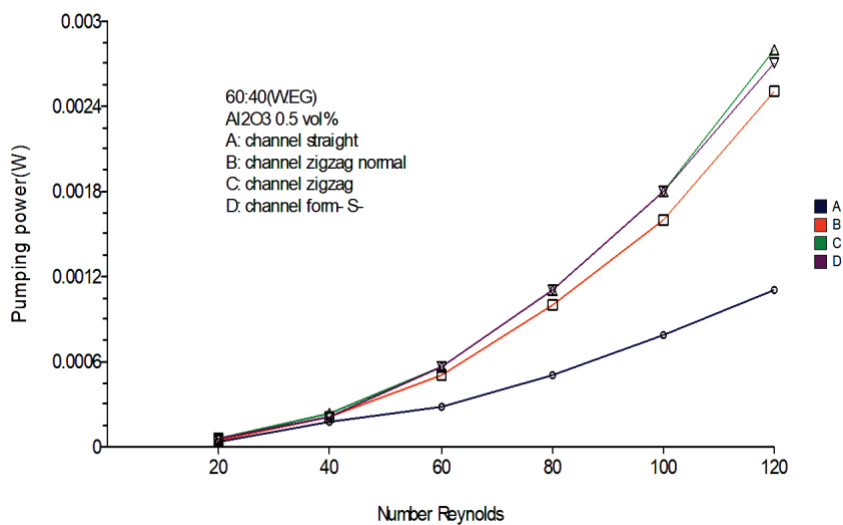


Figure 8. The pumping power of the nanofluid (Al_2O_3 -W (60) / EG (40) mixture) versus Reynolds number.

of Reynolds number of 120 was obtained which 1537.26 Pa compared to straight channel (A). It was followed by the S shaped channel in the form of the letter S (D) with an increase of up to 1464.06 Pa. However, we also observed a high increase for the broken channel in the decrease in pressure estimated at 1260.34 Pa in relation to the straight channel and a large decrease in pressure of the channels (D, C, B). The coolant is affected by the boundaries of the flow channels that obstruct its path between the inlet and outlet.

The effects of pumping energy for flow channels (D, C, B) compared to the normal straight channel (A) at Reynolds greater than 40 are shown in Figure 8. The high pressure decreases for pumping power with fewer generalization of more Al_2O_3 nanoparticles in the cooling system. The curved flow channel (C) at Reynolds number of 120 has resulted in an additional pumping power of 0.00017 W compared to the straight channel, the pumping power of the flow channel –S- (D) for Reynolds 120 was equal to 0.0016 W compared to the straight channel, followed by the broken channel at an addition rate of 0.0014 W. These pumping increases are due to the significant pressure drop between the inlet and outlet of the flow channels (B, C, D). High pumping power demands are not appropriate for the output of fuel cells because this would raise the unnecessary losses associated with the cooling system requirement.

Figure 9 displays a simulation of temperature distribution at the flow channel stage at Reynolds number of 120, where the temperature evolution of the Al_2O_3 nano-coolant in the flow region and the temperature distribution throughout steel plate channel in general are observed. Via the absorption of the reaction energy, the fluid energy decreases around the liquid channels and is therefore highest near the outlet and lowest near the inlet of the coolant liquid zone. It also indicates a small variation in the local nanofluid temperature of the cooling plates with various fluid flow structures.

The role of the cooling plate is to exhaust the reaction heat from PEMFC to avoid overheating as well as leading to maintaining an even temperature distribution in the active area and the most important is the distribution of temperature on the surface of the plate as displayed in Figure 10. It is clear that the flow field design (S) and curve (C, D) give a better cooling device compared to the straight and refracted channel in terms of uniformity of temperature. The straight and refracted flow field (A, B) shows that the high gradient starts from the low level of hotspot near the inlet to a high hotspot near the outlet.

A uniformity temperature index (U_T) is known as the temperature control measurement index for more quantitative analysis of the cooling efficiency. In quantitative words, U_T is the difference of surface temperature T at the heat transfer interface from the average temperature T_{avg} . In other terms, when the temperature distribution is even, U_T is zero.

$$U_T = \frac{\int |T - T_{avg}| dA}{dA} \quad (9)$$

$$T_{avg} = \frac{\int T dA}{dA}$$

Here A is the area, and T_{avg} , T are the average temperature and the temperature of surface, respectively. In this equation, integration is determined only on the heat flow limit.

The results show that the surface temperature uniformity index for the three models matched the results with a slight change of 0.001 compared to the straight channel. The control of hotspot points on the cooling channels surface in order to confirm the heat stability of PEM fuel cell is very requested. In fact, it is the most important parameter in preventing heat damage to the cell. Table 4 and Figure 10 show that the maximum hotspot on the channel surface (S) T_{max} is about 4K less than pattern (A) followed by channel (C) with a decrease of 2.12 K and channel (B) with a decrease of 1.28 K. The T_{avg} mean values for the four designs are identical with little variation in Reynolds number 120 less than the conventional (A) design.

Through the study of the U_T and T_{avg} , no differences have been noticed between them for the flow channels (B,

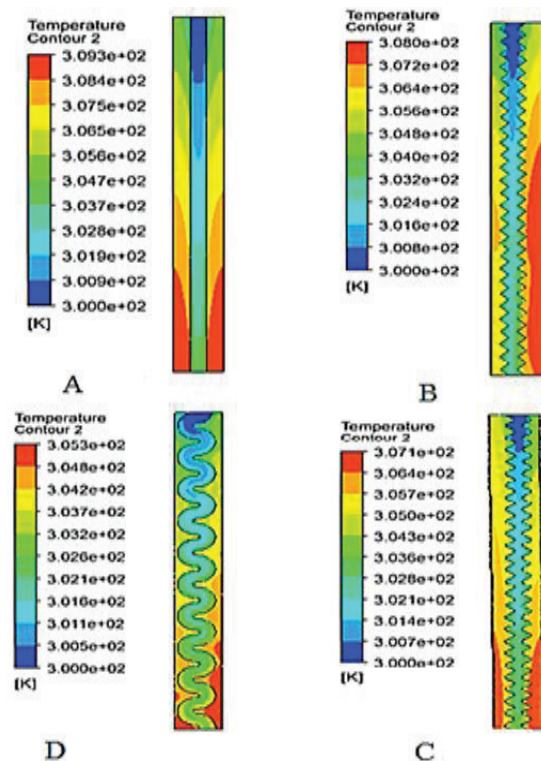


Figure 9. Temperature distribution at the level of nanofluid flow channels for Reynolds number of 120.

Table 4. Numerical results of the four models

Model	$T_{max}(K)$	$T_{min}(K)$	$\Delta T(K)$	AR%
One stage straight plate	309.27	300	9.27	/
normal zigzag plate	307.99	300	7.99	14.1
curved zigzag plate	307.15	300	7.15	7.72
S-shaped plate	305.3	300	5.3	2.21
Two stages straight plate	305.5	300	5.5	/

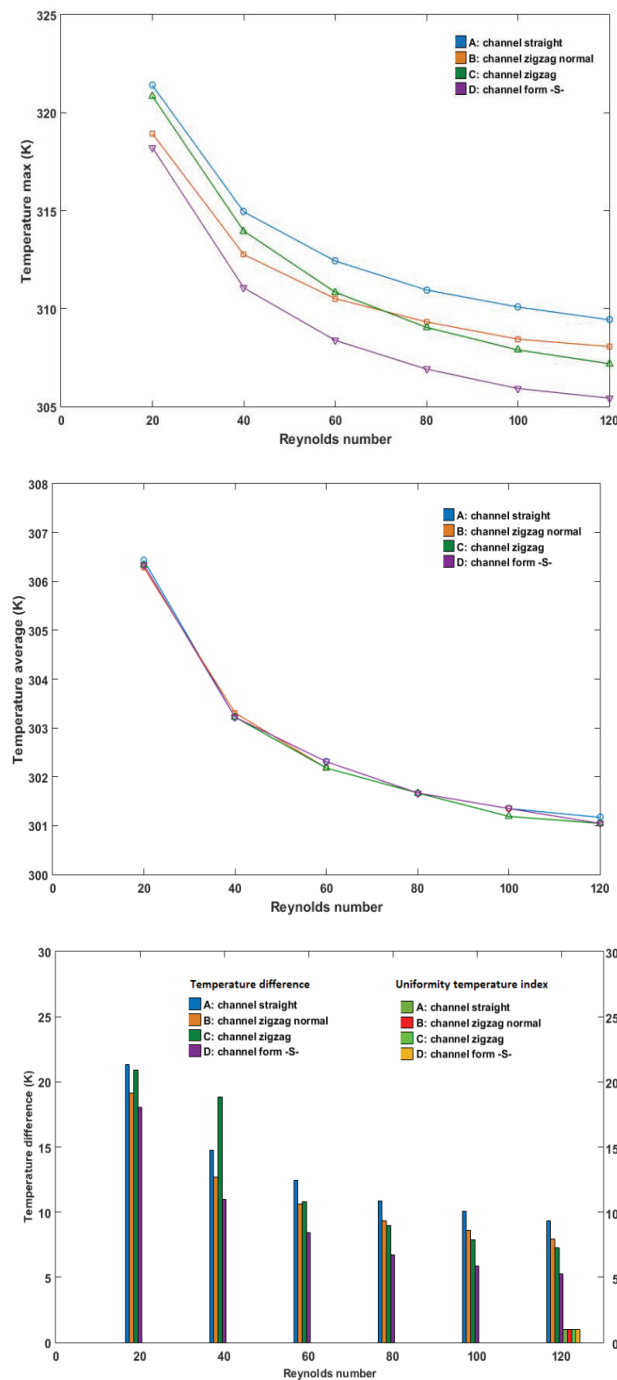


Figure 10. Thermal analysis results of the four models

C, D) compared to (A). Therefore, the advantage ratio was relied to find the most appropriate flow field for the PEMFC fuel cell cooling field given as [29]

$$AR = \frac{h_i - h_A / h_A}{\Delta P_i - \Delta P_A / \Delta P_A}; i = B, C, D \quad (10)$$

For all Al_2O_3 analyzed, the advantage ratio was found to be the strongest in lower Reynolds number. This is attributed to the smaller pressure decrease observed in the lower of Reynolds number as opposed to the higher of Reynolds number although the change in heat transfer stays constant across the total range of Reynolds number [4].

According to Figure 11, the flow channel -S- (D) shows its benefit at Reynolds number of 60 and above so that Reynolds number of 120 reaches the highest interest rate of 14.2% compared to the straight channel. It is followed by the curved channel (C) and the broken channel (B), so that they are useful for Reynolds number of 80 and above, with an advantage ratio of 7.72% and 2.21%, respectively, compared to the straight line.

Figure 12 provides the numerical temperature contours at the wall area for straight plate simple stage, two stages plate with co-current and counter-current fluid flow. The temperature rises along the channel due to the absorption of reaction heat, therefore it is minimum at the entrance and

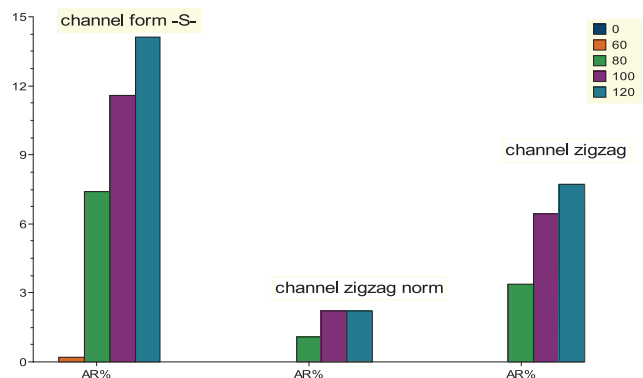


Figure 11. Advantage ratio (AR) for models B, C, and D

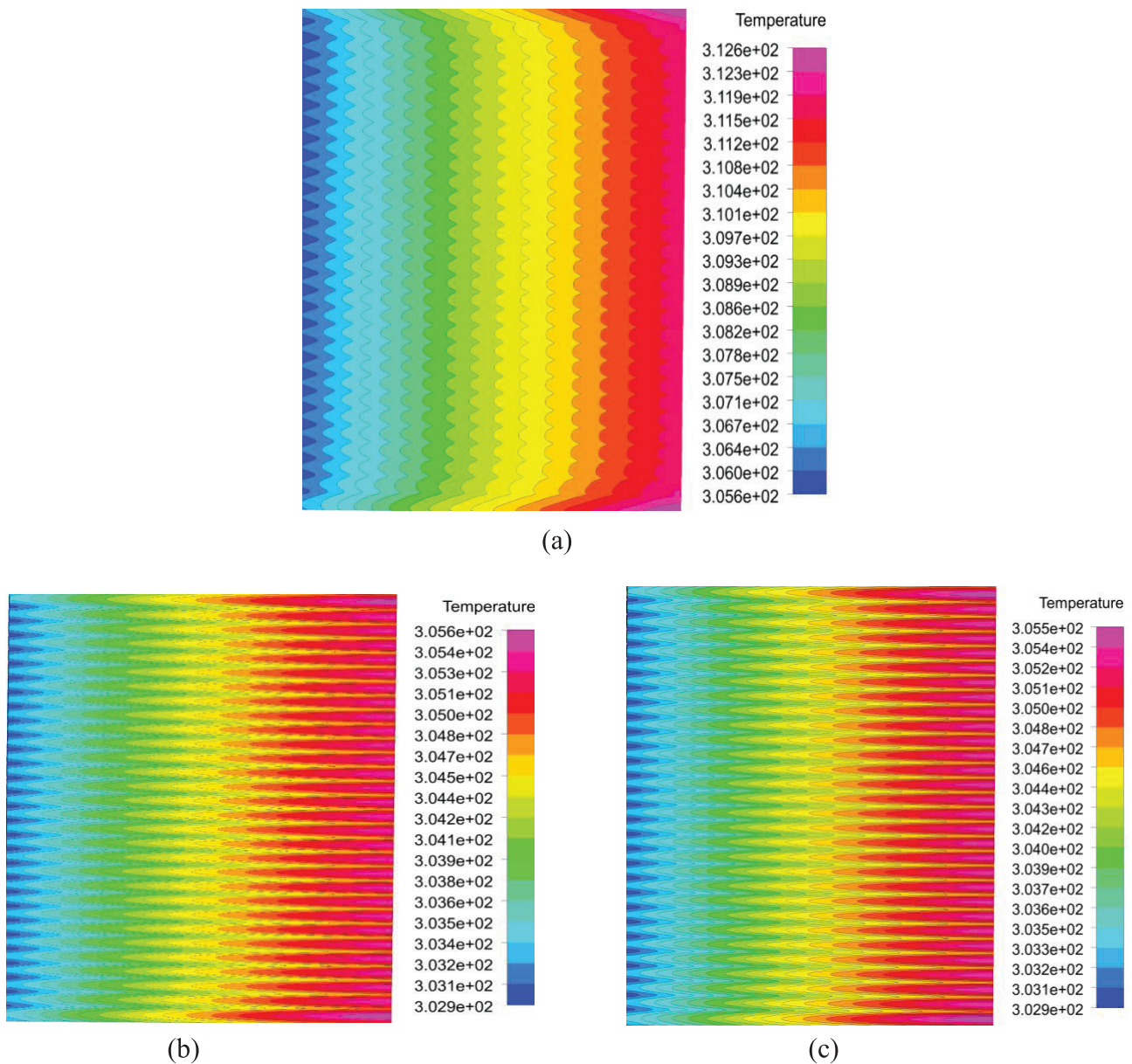


Figure 12. Temperature distribution at the area of wall for three straight plates: a) Straight plate simple, b) two stages Straight plate co-current and c) two stages Straight plate counter-current.

maximum at the outflow of the coolant microchannels. The results show the local hotspot difference is estimated around 312.5 K, 305.5 K, and 305.6 K for straight plate simple, co-current plate and counter-current plate, respectively. The findings reported here suggest that the role of cooling plates is very important in which it prevent the PEMFCs overheating by exhaust heat from chemical reaction.

The temperature distributions of fluids in two stages straight plate for co-current and counter-current cases are studied and compared, as presented in Figure 13. It is clearly seen that in the first stage, which used nanofluids (Al_2O_3 -W / EG Mixture) 0.5%, the maximum temperature reached 305.5 K for two cases co-current and counter-current

while in the second stage which utilized nanofluids (SiO_2 in desalted water) 0.5%, the temperature estimated 312.6 K for co-current and 305.5 K for counter-current. On other hand, there is an increase in temperature and heat distribution in the second stage, and this is due to the increase in the thermal interaction and fluid convective in the channel

CONCLUSIONS

A CFD simulation was performed for the microchannel design impact on the thermal performances of PEMFCs. The nano-fluids used within the channels, along with channels designs, have an essential role in the heat extraction

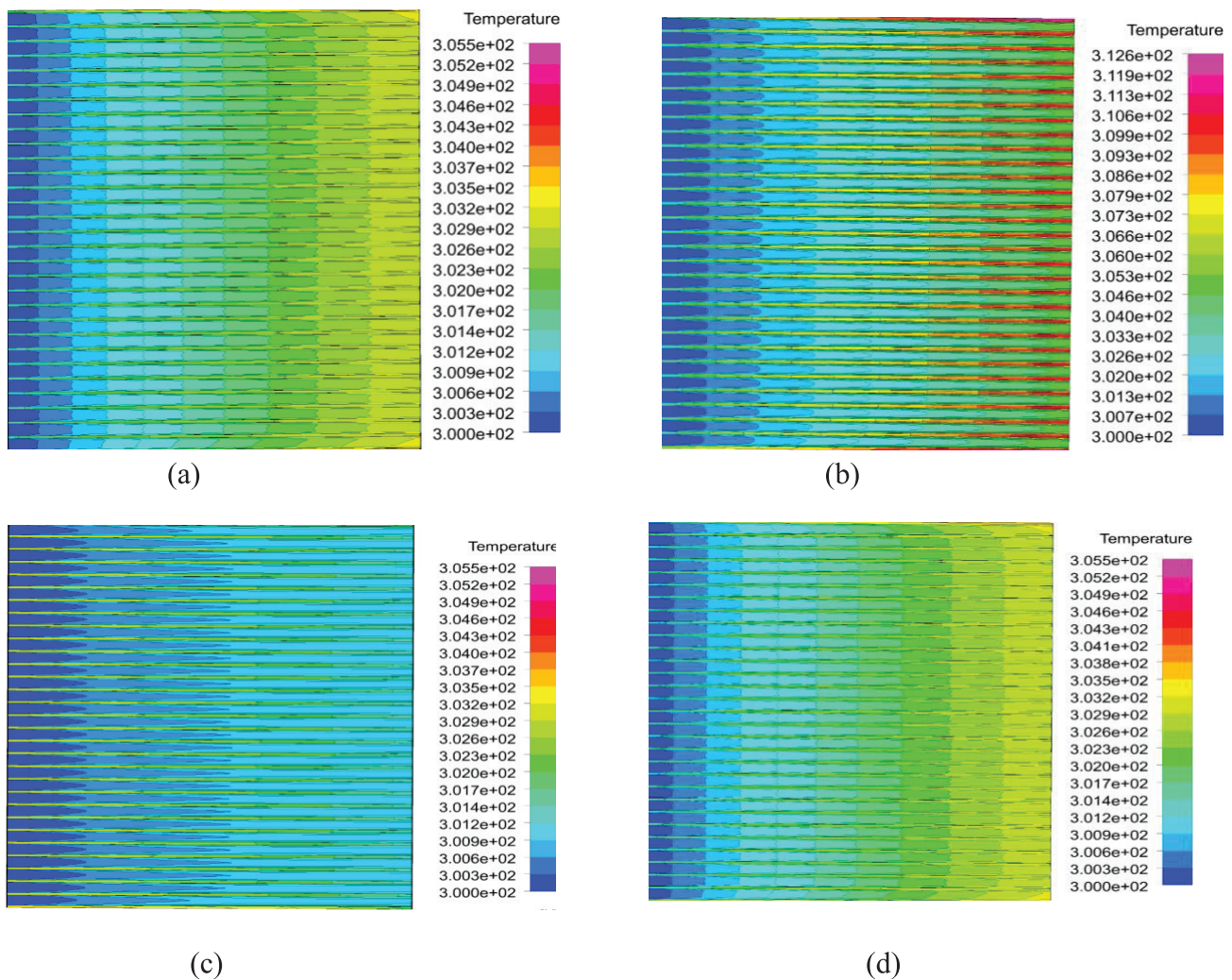


Figure 13. Temperature distribution of fluids in two stages straight plate for co-current and counter-current cases: a) First stage co-current, b) Second stage co-current, c) First stage counter-current, d) Second stage counter-current.

and cooling process of PEM full Cells. The effect of four different cooling flow plate was investigated and compared to the traditional plate (straight microchannel design) according to maximum temperature and temperature uniformity index. This parametric study is necessary when looking for the optimal cooling flow field microchannel designs for effective and uniform cooling system of PEM fuel cells. The found outcomes depicted that the temperature uniformity index, the average surface temperature, the difference and the maximum temperature in S and two stages coolant flow field microchannel designs are lower than conforming results in a straight microchannel model. The shape of the geometry D path causes an increase in the arrival time of the fluid, which resulted in effects on the parameters such as an increase in the value of the convective thermal coefficient at a high value of Reynolds.

The temperature difference of one stage straight plate, S-design, and two stages coolant flow field microchannel

model were obtained and found to be about 9.27 K, 5.3 K and 5.5 K, respectively. Especially in higher heat fluxes and higher coolant flow rates imposed on the coolant plate, the enhancement in the thermal performance of S-design and two stages coolant flow field channels is more significant. Hence, it can be considered that the mentioned models have the potential to be utilize for providing more enhancements to PEMFC compared to other conventional models. However, further study should be conducted about thermal performances and pressure drops to make more developments on these models. The findings reported in the present work suggest that the designing of different cooling plate models for large-scale PEM fuel cells is very recommended. Research questions that could be asked include the heat transfer effect with an electrical part in 3D PEMFC is suggested to be investigated with the application of different boundary conditions.

NOMENCLATURE

A	Area, m ²
h	Convective heat transfer coefficient, W.m ⁻² . K ⁻¹
Q	Flow rate, m ³ .s ⁻¹
x, y, z	Dimension, m
V	Velocity, m.s ⁻¹
T	Temperature, K
μ	Dynamic viscosity of the nanofluid, Pa.s
P	Pressure, Pa
C_p	Specific heat, J.kg ⁻¹ . K ⁻¹
K_{nf}	Thermal conductivity of the nanofluid, W.m ⁻¹ . K ⁻¹
q	Heat flow rate, W.m ⁻²
H_c	Channel depth, m
W_c	Channel width, m
H_p	Plate height, m
W_p	Plate width, m
L_p	Plate length, m
K_s	Thermal conductivity of cooling plate, W.m ⁻¹ . K ⁻¹
U_T	Uniformity temperature index, K
T_{avg}	Average temperature, K
Re	Reynolds number
Nu	Nusselt number

Subscripts

nf	Nanofluid
avg	Average
min	Minimum
max	Maximum

Acronyms

AR	Advantage Ratio
PEMFC	Polymer Electrolyte Membrane Fuel Cell
W/EG	Water/Ethylene Glycol
CFD	Computational Fluid Dynamics

ACKNOWLEDGMENT

This paper was supported by General Directorate of Scientific Research and Technological Development (DGRSDT).

AUTHORSHIP CONTRIBUTIONS

Authors equally contributed to this work.

DATA AVAILABILITY STATEMENT

The authors confirm that the data that supports the findings of this study are available within the article. Raw data that support the finding of this study are available from the corresponding author, upon reasonable request.

CONFLICT OF INTEREST

The author declared no potential conflicts of interest with respect to the research, authorship, and/or publication of this article.

ETHICS

There are no ethical issues with the publication of this manuscript.

REFERENCES

- [1] Gao F, Blunier B, Miraoui A. Proton exchange membrane fuel cells modeling. John Wiley & Sons; 2013. [\[CrossRef\]](#)
- [2] Ozdogan M. Numerical investigation of effects of working conditions on performance of pem fuel cell. J Therm Eng 2019;5:14–24. [\[CrossRef\]](#)
- [3] Lakshminarayanan V, Karthikeyan P. Performance enhancement of interdigitated flow channel of PEMFC by scaling up study. Energy Sources Part A-recovery Utilization and Environmental Effects 2020;42:1785–1796. [\[CrossRef\]](#)
- [4] Pietrosemoli L, Rodríguez-Monroy C. The Venezuelan energy crisis: Renewable energies in the transition towards sustainability. Renew Sust Energy Rev 2019;105:415–426. [\[CrossRef\]](#)
- [5] Bouraiou A, Necaibia A, Boutasseta N, Mekhilef S, Dabou R, Ziane A, et al. Status of renewable energy potential and utilization in Algeria. J Clean Prod 2020;246:119011. [\[CrossRef\]](#)
- [6] Kerkoub Y. Etude de l'effet des paramètres géométriques et opérationnels sur les phénomènes de transport et sur la performance d'une pile à combustible PEMFC. 2019.
- [7] Taner T. A flow channel with nafion membrane material design of PEM fuel cell. J Therm Eng 2019;5:456–468. [\[CrossRef\]](#)
- [8] Spiegel C. PEM fuel cell modeling and simulation using MATLAB. Elsevier; 2011.
- [9] Taner T. The micro-scale modeling by experimental study in PEM fuel cell. J Therm Eng 2017;3:1515–1526. [\[CrossRef\]](#)
- [10] Zakaria IA, Azmin ASMA, Khalid S, Hamzah WAW, Mohamed WANW. Numerical analysis of aluminium oxide and silicon dioxide nanofluids in serpentine cooling plate of PEMFC. J Adv Res Fluid Mech Therm Sci 2020;72:67–79. [\[CrossRef\]](#)
- [11] Khalid S, Zakaria I, Azmi W, Mohamed W. Thermal-electrical-hydraulic properties of Al₂O₃-SiO₂ hybrid nanofluids for advanced PEM fuel cell thermal management. J Therm Anal Calorim 2021;143:1555–1567. [\[CrossRef\]](#)
- [12] Arear W, Zeiny A, Al-Baghdadi MAS. Influence of Al₂O₃-Water Nanofluid Coolant on Thermal Performance of Hydrogen PEM Fuel Cell Stacks. IOP Conf Ser Mater Sci Eng 2021;1094:012064. [\[CrossRef\]](#)
- [13] Johari MNI, Zakaria IA, Azmi W, Mohamed W. Green bio glycol Al₂O₃-SiO₂ hybrid nanofluids for PEMFC: The thermal-electrical-hydraulic perspectives. Int Commun Heat Mass Transf 2022;131:105870. [\[CrossRef\]](#)

- [14] Kordi M, Moghadam AJ, Afshari E. Effects of cooling passages and nanofluid coolant on thermal performance of polymer electrolyte membrane fuel cells. *J Electrochem Energy Convers Storage* 2019;16. [\[CrossRef\]](#)
- [15] Afshari E, Ziaei-Rad M, Jahantigh N. Analytical and numerical study on cooling flow field designs performance of PEM fuel cell with variable heat flux. *Mod Phys Lett B* 2016;30:1650155. [\[CrossRef\]](#)
- [16] Saeedan M, Afshari E, Ziaei-Rad M. Modeling and optimization of turbulent flow through PEM fuel cell cooling channels filled with metal foam—a comparison of water and air cooling systems. *Energy Convers Manage* 2022;258:115486. [\[CrossRef\]](#)
- [17] Mahdavi A, Ranjbar AA, Gorji M, Rahimi-Esbo M. Numerical simulation based design for an innovative PEMFC cooling flow field with metallic bipolar plates. *Appl Energy* 2018;228:656–666. [\[CrossRef\]](#)
- [18] Idris MS, Zakaria IA, Hamzah WAW, Mohamed WANW. The Characteristics of Hybrid Al₂O₃: SiO₂ Nanofluids in Cooling Plate of PEMFC. *J Adv Res Fluid Mech Therm Sci* 2021;88:96–109. [\[CrossRef\]](#)
- [19] Ogura N, Kawamura Y, Yahata T, Yamamoto K, Terazaki T, Nomura M, et al. Small PEMFC system with multi-layered microreactor. *IEEJ Trans Sens Micromach* 2006;126:54–59. [\[CrossRef\]](#)
- [20] Chugh S, Chaudhari C, Sonkar K, Sharma A, Kapur G, Ramakumar S. Experimental and modelling studies of low temperature PEMFC performance. *Int J Hydrogen Energy*.
- [21] Lu J, Wei G, Zhu F, Yan X, Zhang J. Pressure Effect on the PEMFC Performance. *Fuel Cells* 2019;19:211–220. [\[CrossRef\]](#)
- [22] Chun JH, Park KT, Jo DH, Kim SG, Kim SH. Numerical modeling and experimental study of the influence of GDL properties on performance in a PEMFC. *Int J Hydrogen Energy*. 2011;36:1837–1845. [\[CrossRef\]](#)
- [23] Vijayakrishnan MK, Palaniswamy K, Ramasamy J, Kumaresan T, Manoharan K, Rajagopal TKR, et al. Numerical and experimental investigation on 25 cm² and 100 cm² PEMFC with novel sinuous flow field for effective water removal and enhanced performance. *Int J Hydrogen Energy* 2020;45:7848–7862. [\[CrossRef\]](#)
- [24] Zakaria I, Azmi W, Mamat A, Mamat R, Saidur R, Talib SA, et al. Thermal analysis of Al₂O₃-water ethylene glycol mixture nanofluid for single PEM fuel cell cooling plate: an experimental study. *Int J Hydrogen Energy* 2016;41:5096–5112. [\[CrossRef\]](#)
- [25] Afshari E, Ziaei-Rad M, Dehkordi MM. Numerical investigation on a novel zigzag-shaped flow channel design for cooling plates of PEM fuel cells. *J Energy Inst* 2017;90:752–763. [\[CrossRef\]](#)
- [26] Baek SM, Yu SH, Nam JH, Kim C-J. A numerical study on uniform cooling of large-scale PEMFCs with different coolant flow field designs. *Appl Thermal Eng* 2011;31:1427–1434. [\[CrossRef\]](#)
- [27] Li S, Sundén B. Numerical study on thermal performance of non-uniform flow channel designs for cooling plates of PEM fuel cells. *Numer Heat Transf Part A Appl* 2018;74:917–930. [\[CrossRef\]](#)
- [28] Authayanun S, Saebea D, Patcharavorachot Y, Assabumrungrat S, Arpornwichanop A. Optimal design of different reforming processes of the actual composition of bio-oil for high-temperature PEMFC systems. *Int J Hydrogen Energy* 2017 Jan 26;42:1977–1988. [\[CrossRef\]](#)
- [29] Hashmi SMH. Cooling strategies for PEM FC stacks. 2010.